

Transmission properties of terahertz pulses through subwavelength double split-ring resonators

Abul K. Azad, Jianming Dai, and Weili Zhang

School of Electrical and Computer Engineering, Oklahoma State University, Stillwater, Oklahoma 74078

Received August 18, 2005; revised October 28, 2005; accepted November 1, 2005

We present a terahertz time-domain spectroscopy study of the transmission properties of planar composite media made from subwavelength double split-ring resonators (SRRs). The measured amplitude transmission spectra reveal a resonance near 0.5 THz, the central frequency of most ultrafast terahertz systems, for one SRR orientation in normal-incidence geometry. This resonance is attributed to the effect of electric excitation of magnetic resonance of the SRR arrays. In addition, the influences of background substrate, lattice constant, and the shapes of the SRRs on the terahertz resonance are experimentally investigated and agree well with the results of recent numerical studies. © 2006 Optical Society of America
OCIS codes: 320.7120, 160.4670.

The existence of negative index materials (NIMs) was experimentally demonstrated in the microwave region by Smith *et al.*,¹ who combined Pendry's metal wires and split-ring resonators (SRRs) in a composite structure, enabling the effective permittivity ϵ_{eff} and permeability μ_{eff} to be simultaneously negative.¹⁻³ NIMs will open up an entirely new world of devices that will affect broad areas, such as communications, data storage, lithography, and biomedical imaging. Recently, there has been an emerging interest in tuning the resonance frequencies of NIMs to the terahertz and infrared regions.⁴⁻⁸ At terahertz frequencies, Yen *et al.* achieved magnetic response at 0.8–1.3 THz in the planar microstructured SRR composites as measured by spectroscopic ellipsometry.⁴ Very recently, Katsarakis *et al.* demonstrated magnetic resonance near 6 THz in a multilayer composite made from single-ring SRRs.⁸ In this Letter we present experimentally determined transmission properties of planar subwavelength double-ring SRR arrays characterized by terahertz time-domain spectroscopy (THz-TDS) in the frequency range from 0.1 to 3.5 THz. Various arrays made from square and circular double-ring SRRs were lithographically fabricated for experimental investigation of the effects of background substrate, lattice constant, and the shape of the SRRs on the transmission properties of terahertz pulses in normal-incidence geometry. In one of the SRR orientations a resonance near 0.5 THz was observed in a double-ring SRR array patterned on silicon and disappeared when the splits of the rings were closed. This resonance is interpreted in terms of the effect of electric excitation of magnetic resonance when the incident terahertz pulses are polarized perpendicular to the splits of the SRRs and penetrate the array at normal incidence.^{5,8-11}

As an effective magnetic element, the SRR usually has either a square or a circular configuration, as shown in Figs. 1(a) and 1(b), respectively. A double-ring SRR consists of two concentric split rings situated oppositely and made from conductive material. The function of the splits is to allow the SRR unit to be resonant at wavelengths much longer than the physical dimension of the rings.¹ The small split ring inside the unit enables a capacitance to be formed be-

tween the rings. As a result, the resonance frequency is lower than that of the outer single-ring SRR, and this facilitates the occurrence of a magnetic response in the negative permeability region of the combined system of SRRs and wires.¹¹

The microstructured SRR array is an optically thick 200 nm aluminum layer lithographically fabricated on either silicon (0.64 mm thick, *p*-type resistivity 20 Ω cm) or fused quartz (1.03 mm thick) substrates. Figures 1(c) and 1(d) show microscopic images of the square and circular SRR arrays, respectively. The square and circular SRRs have essentially the same linear dimensions, with a minimum feature of $d=2 \mu\text{m}$ in the splits of the rings and a submicrometer resolution. The clear aperture of the samples is 20 mm \times 20 mm, which is large enough for either focused or parallel beam THz-TDS character-

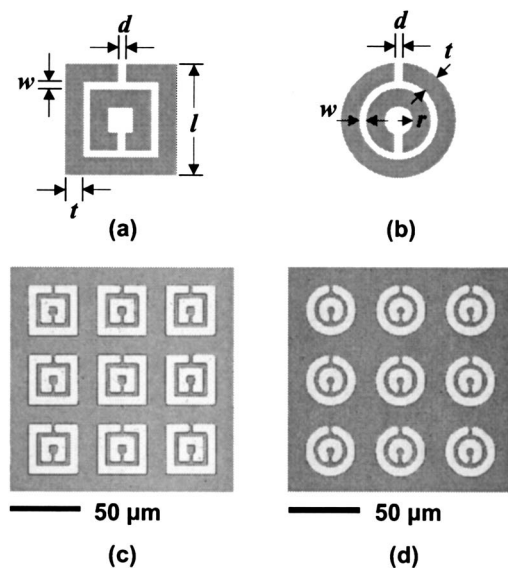


Fig. 1. Diagrams of (a) a square SRR and (b) a circular SRR. (c) Microscopic image of a square SRR array made from aluminum on silicon; the dimensions of the SRR are $d=2 \mu\text{m}$, $w=3 \mu\text{m}$, $t=6 \mu\text{m}$, $l=36 \mu\text{m}$, and lattice constant $P=50 \mu\text{m}$. (d) Image of a circular SRR array with the same dimensions as those of the square SRR array with $r=3 \mu\text{m}$.

ization. The physical parameters of the SRR are determined based on recent numerical results,^{4,11} so the SRR can be magnetically resonant at 0.5 THz. Typically, this frequency corresponds to the peak of the amplitude spectrum in ultrafast terahertz systems and is one at which extensive applications have been demonstrated, particularly in imaging, ranging, and interconnects.^{12–14}

Terahertz spectroscopic characterization of the SRR arrays is undertaken by use of a broadband, photoconductive switch-based THz-TDS system.^{15,16} THz-TDS has shown significant advantages in material characterization, particularly because transmitted coherent terahertz pulses provide a high signal-to-noise ratio and significant time-resolved phase information. The THz-TDS setup employed here has an 8F confocal geometry¹² and a 3.5 mm frequency-independent beam waist that covers more than 3800 SRRs for lattice constant $P=50 \mu\text{m}$.

Figure 2 illustrates the frequency-dependent amplitude transmission and the phase change of a square-SRR array with a spectral resolution of 0.03 THz. The SRR is oriented with the splits perpendicular to the terahertz electric field; we define this as the perpendicular orientation. In contrast, the parallel orientation is defined when the splits are parallel to the electric field. The transmission is extrapolated from the ratio of the Fourier-transformed amplitude spectra of the sample to the reference, which is a blank slab identical to the substrate of the SRRs. As shown in Fig. 2(a), two distinct resonance features are observed for each SRR array. Since the incident magnetic field is parallel to the plane of the SRRs, both the parallel and the perpendicular orientations were expected to be magnetically inactive.^{10,11} However, recent experimental and theoretical work indicates that an oscillating resonant current can be excited due to the coupling of the electric field to the SRRs in the perpendicular orientation shown in Fig. 2.^{5,8–11} This is referred to as the electric excitation of the magnetic resonance effect that leads to a magnetic response. The phase change is obtained from the phase difference between the sample and the reference spectra. As shown in Fig. 2(b), the phase change has the derivative shape of the sharp resonances observed in the transmission. This shows the consistency of both the measured phase and the amplitude transmission.

Terahertz transmission properties of the square SRR array patterned on both silicon and quartz substrates are compared. In recent work, a magnetic resonance centered at $\omega_m/2\pi=0.82$ THz was demonstrated in a double-ring SRR array on quartz with the same linear dimensions as shown in Fig. 1(c) when a component of the magnetic field penetrated the rings.⁴ Similarly, we observed a low-frequency resonance located at 0.80 THz as indicated by the dotted curves in Fig. 2 but in the normal-incidence geometry where the magnetic field has no component normal to the SRR plane. This stop band is expected for the inductor–capacitor circuit (LC) resonance because of the electric excitation of the magnetic resonance effect.^{5,8–11} To confirm our result, the SRR ar-

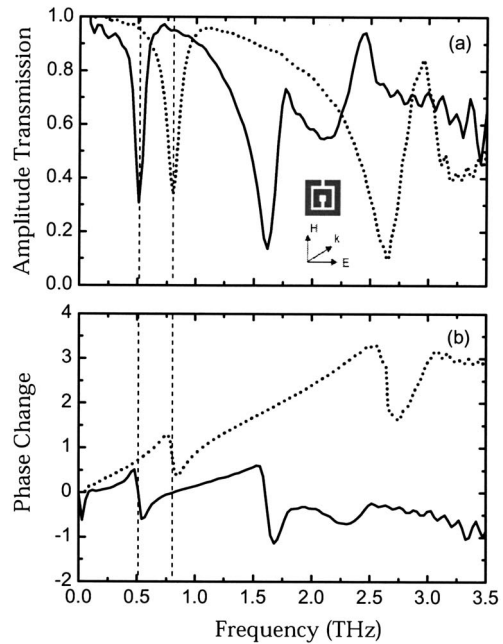


Fig. 2. (a) Measured amplitude transmission and (b) the corresponding phase change of the square SRRs [Fig. 1(c)]: array on silicon, solid curves; array on quartz, dotted curves. The vertical dashed lines indicate the magnetic resonances.

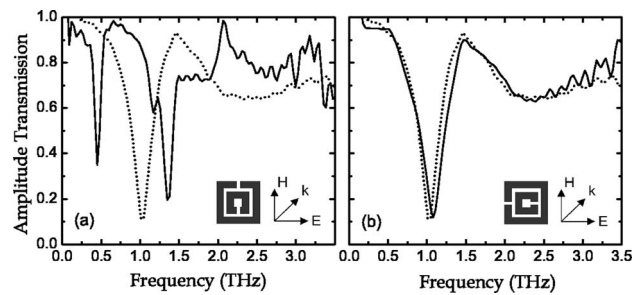


Fig. 3. Measured amplitude transmission of a square SRR array (solid curves) and a CR array (dotted curves) on silicon with the same dimensions: $w=t=5 \mu\text{m}$, $l=40 \mu\text{m}$, and $P=60 \mu\text{m}$, except that $d=5 \mu\text{m}$ for SRR and $d=0$ for CR. (a) Perpendicular orientation, (b) parallel orientation.

ray was vertically angled up to 45° in the terahertz beam path to produce a component of the magnetic field normal to the plane of the SRRs.⁴ However, no frequency shift occurred at the measured resonance of 0.80 THz. Moreover, the metal thickness of the SRR was increased to $2 \mu\text{m}$, but no considerable change was observed in the transmission properties either.

The low-frequency resonance of the SRRs patterned on silicon shifts to the lower frequency of 0.51 THz, as shown by the solid curve in Fig. 2(a). This result is reasonably consistent with the dependence of magnetic resonance frequency on the dielectric constant of the substrate $\omega_m \propto 1/\sqrt{\epsilon_b}$,¹¹ where ϵ_b is the dielectric constant of the background substrate: $\epsilon_b=11.35$ for silicon and $\epsilon_b=3.82$ for fused quartz.¹⁷ However, when the background substrate becomes orders of magnitude thinner than the resonance wavelength, this scaling rule may not be valid in the terahertz region. Further numerical and experimen-

tal studies are needed for a quantitative understanding of this effect.

To further determine the electromagnetic properties of the observed resonance features, we fabricated a pair of arrays composed of SRRs and closed rings. The closed ring has linear dimensions identical to those of the SRR, except that $d=0$. As shown in Fig. 3, the amplitude transmission of the closed rings depicted by the dotted curves reveals a single stop band that almost completely overlaps the resonance for the SRR array in parallel orientation. Clearly, the low-frequency resonance observed in the perpendicular orientation is removed by closing the splits in the rings, while the second resonance at 1.35 THz shifts to the lower frequency and overlaps the stop band for parallel orientation. According to previous studies,^{5,8–11,18} the low-frequency resonance, in this case at 0.50 THz, is further confirmed as the magnetic response. The resonance for parallel orientation in Fig. 3(b) and the second resonance at relatively higher frequencies for perpendicular orientation in Figs. 2(a) and 3(a) are attributed primarily to the electric response of the SRRs.

In Fig. 4(a) we show the dependence of the SRR resonances on the lattice constant. Two circular SRR arrays that employ the same SRR unit as shown in Fig. 1(b) were fabricated, with lattice constants of 50 and 60 μm . As expected, the position of the low-frequency resonance at 0.59 THz does not shift with respect to the lattice constant.⁵ The reduced strength and linewidth with increasing lattice constant are due to the smaller number density of the SRRs per unit area, such that the total contribution of the SRRs and the interaction between the SRRs are reduced. In addition, the transmission properties of the terahertz pulses from square and circular SRR arrays have been compared. The two arrays have identical linear dimensions [Figs. 1(c) and 1(d)], aluminum layers, and silicon substrates. As shown in Fig. 4(b), the resonance frequencies of the circular SRRs

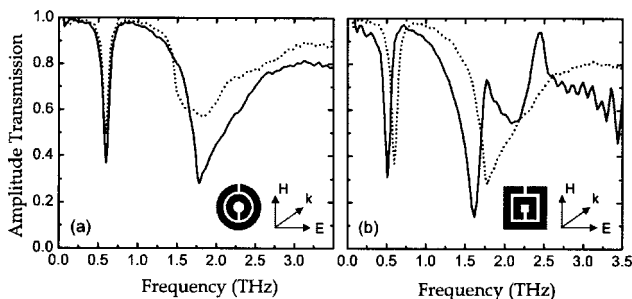


Fig. 4. (a) Measured amplitude transmission of circular SRR arrays on silicon with the same SRR but different lattice constants [Fig. 1(d)] with $P=50 \mu\text{m}$ (solid curve) and $P=60 \mu\text{m}$ (dotted curve). (b) Comparison of amplitude transmission of the square SRR array [Fig. 1(c), solid curve] with the circular SRR array [Fig. 1(d), dotted curve], both on silicon.

are higher than those of the square SRRs. The low-frequency resonance is centered at 0.59 THz for the circular SRRs and at 0.51 THz for the square SRRs. This difference is due to the fact that the circular SRR has a smaller area than the square SRR of the same linear dimensions. The resonance frequency is inversely proportional to the square root of SRR area $\omega_m \propto 1/\sqrt{A}$, where A is the area occupied by a SRR.¹¹

We thank John O'Hara and Qirong Xing for stimulating discussions. This work was partially supported by the Oklahoma Experimental Program to Stimulate Competitive Research for the National Science Foundation. J. Dai is now with the Rensselaer Polytechnic Institute. W. Zhang's e-mail address is wvwzhang@okstate.edu.

References

1. D. R. Smith, W. J. Padilla, D. C. Vier, S. C. Nemat-Nasser, and S. Schultz, *Phys. Rev. Lett.* **84**, 4184 (2000).
2. J. B. Pendry, A. Holden, W. Stewart, and I. Youngs, *Phys. Rev. Lett.* **76**, 4773 (1996).
3. J. B. Pendry, A. Holden, D. D. Robbins, and W. Stewart, *IEEE Trans. Microwave Theory Tech.* **47**, 2075 (1999).
4. T. J. Yen, W. J. Padilla, N. Fang, D. C. Vier, D. R. Smith, J. B. Pendry, D. N. Basov, and X. Zhang, *Science* **303**, 1494 (2004).
5. S. Linden, C. Enkrich, M. Wegener, J. Zhou, Th. Koschny, and C. M. Soukoulis, *Science* **306**, 1351 (2004).
6. S. Zhang, W. Fan, A. Frauenglass, B. Minhas, K. J. Malloy, and S. R. J. Brueck, *Phys. Rev. Lett.* **94**, 037402 (2005).
7. L. Alekseyev, V. A. Podolskiy, and E. E. Narimanov, in *CLEO/QELS/PhAST'2005 Technical Digest* (Optical Society of America, 2005), CD-ROM, paper JThC2.
8. N. Katsarakis, G. Konstantinidis, A. Kostopoulos, R. S. Penciu, T. F. Gundogdu, M. Kafesaki, E. N. Economou, Th. Koschny, and C. M. Soukoulis, *Opt. Lett.* **30**, 1348 (2005).
9. P. Gay-Balmaz and O. J. Martin, *J. Appl. Phys.* **92**, 2929 (2002).
10. N. Katsarakis, Th. Koschny, M. Kafesaki, E. N. Economou, and C. M. Soukoulis, *Appl. Phys. Lett.* **84**, 2943 (2004).
11. M. Kafesaki, T. Koschny, R. S. Penciu, T. F. Gundogdu, E. N. Economou, and C. M. Soukoulis, *J. Opt. A Pure Appl. Opt.* **7**, S12 (2005).
12. B. Ferguson and X.-C. Zhang, *Nat. Mater.* **1**, 26 (2002).
13. R. A. Cheville, R. W. McGowan, and D. Grischkowsky, *IEEE Antennas Propag.* **45**, 1518 (1997).
14. S. Coleman and D. Grischkowsky, *Appl. Phys. Lett.* **83**, 3656 (2003).
15. D. Qu, D. Grischkowsky, and W. Zhang, *Opt. Lett.* **29**, 896 (2004).
16. D. Qu and D. Grischkowsky, *Phys. Rev. Lett.* **93**, 196804 (2004).
17. D. Grischkowsky, S. Keiding, M. van Exter, and Ch. Fattinger, *J. Opt. Soc. Am. B* **7**, 2006 (1990).
18. K. Aydin, K. Guven, M. Kafesaki, L. Zhang, C. M. Soukoulis, and E. Ozbay, *Opt. Lett.* **29**, 2623 (2004).